BUILDING RECONSTRUCTION FROM HIGH-RESOLUTION INSAR DATA OF URBAN AREAS

U. Stilla, U. Soergel, U. Thoennessen

FGAN-FOM Research Institute for Optronics and Pattern Recognition
76275 Ettlingen, Germany
stilla@fom.fgan.de

The improved ground resolution of state of the art synthetic aperture radar (SAR) sensors suggests to use this technique for the analysis of urban areas. The quality of 3D reconstruction of buildings from SAR or InSAR data is limited by phenomena caused from the inherent oblique scene illumination of SAR sensors. Geometric constraints of the impact of the mentioned SAR phenomena on the visibility of buildings are derived. In this paper an approach for the detection and reconstruction of buildings from an InSAR data set is proposed. The analysis is carried out in an iterative manner. Intermediate results are used as a basis for simulations of InSAR data. The simulation results are compared with the real imagery. Deviations between the simulations and the real data are eliminated step-by-step. The approach is demonstrated for an InSAR data set of a building group in an urban area.

1 Introduction

The increasing resolution of SAR sensors opens the possibility to utilize such data for scene interpretation in urban areas. Approaches for 3D building recognition from SAR and InSAR data have been proposed for rural areas [Bolter, 2001], industrial plants [Soergel, 2000] and inner city areas with high buildings [Gamba et al., 2000]. As a result it was seen that different SAR specific phenomena [Schreier, 1993] like foreshortening, layover, shadow and multipath-propagation burden the scene interpretation or make it even impossible. These phenomena arise from the side-looking scene illumination of SAR sensors. The mentioned methods from the literature achieved good results for rural areas or large and detached buildings. Especially in dense built-up areas with high buildings, large portions of the data can be interfered by the illumination effects.

However, even in dense urban environment a building recognition is feasible, if the typical appearance of buildings in the data is properly modeled. It is possible to determine the height and the roof structure from the length and the size of the occluded shadow area cast from the building on the ground behind. Other hints to

buildings are layover areas and bright double-bounce scatterers at the building footprint. Such context knowledge is exploited by a novel model-based iterative approach to detect and reconstruct buildings.

2 InSAR data

Side-looking SAR sensors are mounted on satellites or airplanes. The basic sensor principle is to illuminate large areas on the ground with the radar signal and to sample the backscatter. From the different time-of-flight of the incoming signal the range between the sensor and the scene objects is obtained. The analysis of single SAR images is usually restricted to the signal amplitude.

SAR interferometry (InSAR) benefits from the coherent SAR measurement principle. For airborne single-pass across-track interferometry measurements two antennas are mounted perpendicular to the carrier track with a geometric displacement. One antenna illuminates the scene and both antennas receive the backscattered complex signals. An interferogram is calculated using a pixel by pixel complex multiplication of the master signal with the complex conjugated

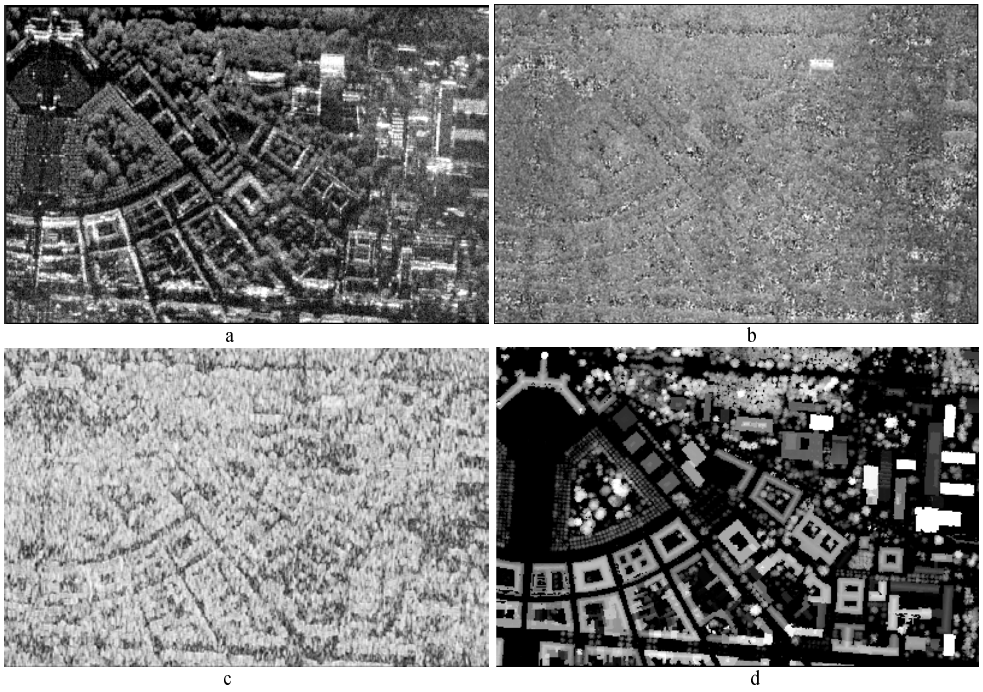

Figure 1. a) intensity, b) height, c) coherence (bright = good), d) LIDAR DEM (ground truth).

slave signal. Due to the geometric displacement, the distances from the antennas to the scene differ, which results in a phase difference in the interferogram. Considering the distance, wavelength, antenna geometry, and viewing angle the elevation differences can by calculated from the phase difference.

The accuracy of a DEM produced with the InSAR technique varies locally depending on the signal to noise ratio (SNR). The so called coherence is a measure of the local SNR. Coherence is usually estimated from the data by a window-based computation of the magnitude of the complex cross-correlation coefficient of the SAR images. The noise sensitivity results often in data holes or competing elevation values after the geocoding with the forward transformation. Hence, the InSAR height data has to be further processed before the geocoding step is carried out.

Fig. 1 illustrates the InSAR data set of the test site in ground range projection and a LIDAR DEM for comparison. The data were recorded by the airborne AER-II experimental multi-channel SAR system [Ender, 1998]. This system has been tested in several flight campaigns on board of a Transall airplane and is equipped with a phased array antenna and several receiver channels. The center frequency of this X-band system is 10 GHz (λ = 3cm) with bandwidth of 160 MHz. The ground range data has a approximate resolution of 1m x 1m. Range direction is from top to down. Assuming a constant noise power, it is evident that in areas with low backscatter power the SNR is poor. This results in a low coherence (Fig. 1c) and distorted height data (Fig. 1b).

3. Appearance of buildings in SAR images

3.1 Phenomena caused by side-looking illumination

Typical effects in SAR images in the vicinity of buildings are illustrated in Fig. 2. The so-called layover phenomenon (Fig. 2a) occurs at locations with steep elevation gradient facing towards the sensor, like vertical building walls. Because object areas located at different positions have the same distance to the sensor, like roofs (I), walls (II) and the ground in front of buildings (III), the backscatter is integrated to the same range cell. Layover areas appear bright in the SAR image.

Perpendicular alignment of buildings to the sensor leads to strong signal responses by double-bounce scattering at the dihedral corner reflector between the ground and the building wall (Fig. 2b). This results in a line of bright scattering in the azimuth direction at the building footprint (Fig. 2c). The gabled roof of the building sketched in Fig. 3 is oriented perpendicular to the sensor. At the opposite building side the ground is partly occluded from the building shadow. This region appears dark in the SAR image, because no signal returns into the related range bins.

Roof structures may lead to strong signal response as well. Since the entire power is mirrored back to the sensor this reflection leads to a line of dominant scattering in azimuth direction, similar to the corner reflector. This bright line caused from the roof appears closer to the sensor in the SAR image compared to the corner reflector. Besides the offset in range direction both effects can be discriminated by their polarimetric properties (single-bounce and double-bounce).

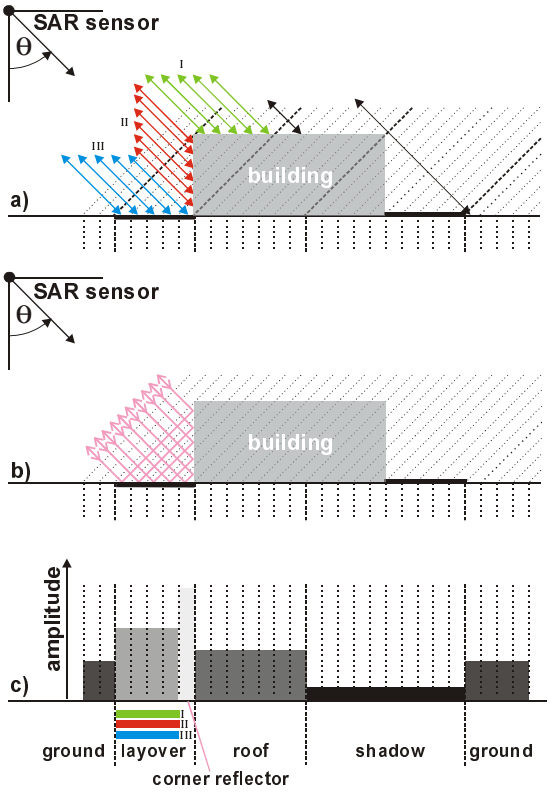

Figure 2. SAR Phenomena at a flat roofed building: a) layover, b) corner reflector, c) range line of SAR image.

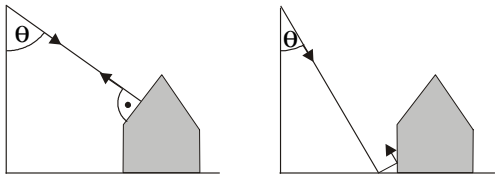

Figure 3. Single (left) and double-bounce scattering at a gabled roof building.

The mentioned effects can be studied in Fig. 4 comparing a section of an aerial image and a SAR image (the castle at the upper left side in Fig. 1). The SAR image is superimposed with the building footprints from a map. The scene was illuminated from top. The signal from the corner reflector at the castle's main building is located at the building footprint (1). The bright signal from the gabled roof is projected on the terrace in front of the castle (2). These two lines enclose the

layover area. Layover can be observed as well at the castle wing (3) and at the tower (4). No line of bright scattering appears at the wing, because the double-bounce signal is reflected away from the sensor. Another double-bounce event happens at a little wall on the border of the terrace (5).

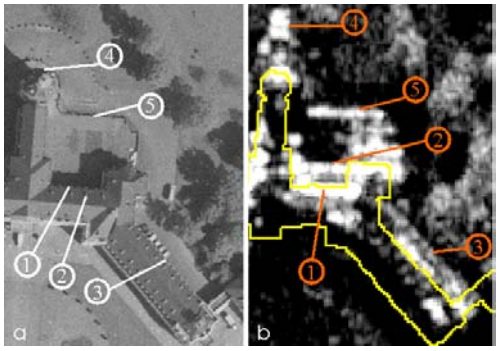

Figure 4. Karlsruhe Castle: a) aerial image (1 main building wall, 2 main building roof, 3 wing, 4 tower, 5 terrace wall), b) SAR image overlaid with building footprints (yellow) and pointers to SAR phenomena (orange), SAR illumination from top to down

3.2 Geometric Constrains

In the following the phenomena of layover and shadow are discussed in more detail. The sizes of the layover areas l_g and shadow areas s_g on the ground in range direction depend on the viewing angle θ and the building height h. The layover area (see Fig. 5a) is given by:

$$l_g = h \cdot \cot(\theta). \quad (1)$$

For the buildings analysis the roof area l_{rt} is of interest which is influenced by layover. At the far side of a building with width w a part of the roof is not interfered with layover (shown in green in Fig. 5a), if the inequation is fulfilled:

$$h < w \cdot \tan(\theta). \quad (2)$$

In case of shadow, geometric relations can be obtained as well (Fig. 5b). The slant range shadow length Δr is the hypotenuse of the right-angeled triangle with the two sides h and s_g. Hence, the building elevation h is given by:

$$h = \Delta r \cdot \cos(\theta). \quad (3)$$

A simple projection of the slant range SAR data on a flat ground plane (ground range), ignoring the building elevation, leads to a wrong mapping of the roofs edge r_1 to point r_1'. Starting from point r_2 the true position x_1 of the building wall can be determined:

$$x_2 = r_2 \cdot \sin(\theta) \quad (4)$$

$$x_1 = x_2 - \Delta r \cdot \sin(\theta) \quad (5)$$

$$s_g = x_2 - x_1 = h \cdot \tan(\theta). \quad (6)$$

However, the shadow analysis is only reliable in a flat ground behind the building and if no signal of other elevated objects interferes with the shadow area (e.g. a neighbored building). It is obvious, that at building locations a steep viewing angle θ leads to large layover areas on the ground and the roofs, but to small

shadow areas and vice versa. Therefore, the viewing angle has to be chosen carefully in order to maximize the portion of useful SAR data.

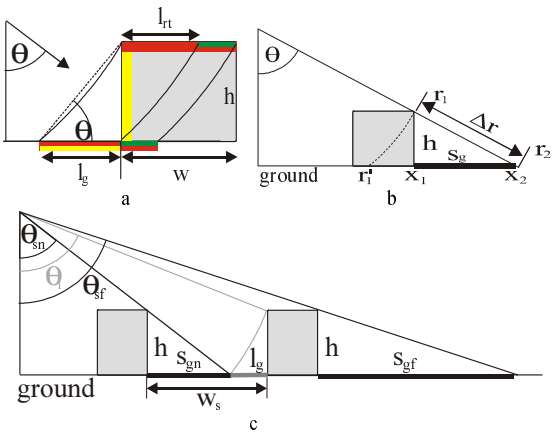

Figure 5. a) Layover in front and on a flat roofed building, b) Shadow behind a building, c) Shadow and Layover from buildings displaced in range direction.

The viewing angle increases in range direction over the swath. Assuming a viewing angle range between 40 and 60 degrees, the shadow length of a certain building is more than doubled from near to far range. In Fig. 5c such a situation is depicted (shadow length s_{gn}, s_{gf}). In the worst case a road between two building rows is orientated parallel to the sensor trajectory. The street is partly occluded from shadow and partly covered with layover. An object on the road can only be sensed properly, if a condition for the road width w_s holds:

$$w_s > s_{gn} + l_g = h \cdot (\tan(\theta_{sn}) + \cot(\theta_l)) \qquad (7)$$

3.3. Simulation of layover, shadow and dominant scattering at buildings

Based on a ground truth DEM (see Sec. 4.1), it is possible to simulate layover and shadow areas [Meier et al., 1993]. Such a simulation was carried out for the test site according to the given parameters of the real SAR data. The result is illustrated in Fig. 6a. A detailed visibility analysis [Soergel et al., 2002] reveals that only 20% of the road area and 43% of the roof area can be sensed properly with

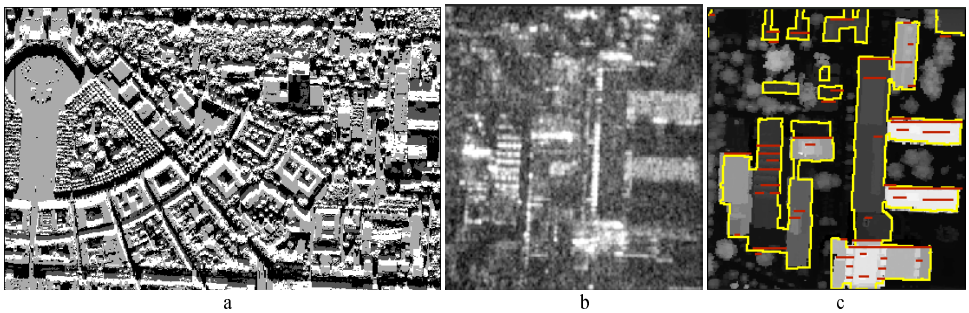

a b c

Figure 6. a). Simulation with the given SAR parameters (range from top to down): Layover (white), shadow (black), layover and shadow (dark grey) and reliable data (bright), b) SAR image of scene detail on the right, c) DEM with building footprints (yellow) and possible corner structures (red).

this SAR measurement. The rest is interfered with layover, shadow or both. Fig. 6b shows detail of the test data with a strong signal at building locations. A fusion of complementing SAR data acquired from different aspects offers the opportunity to fill occluded areas and to correct layover artifacts. The possible locations of strong scattering (red lines in Fig. 6c) were detected by the analysis of 3D vector data derived from the LIDAR DEM [Stilla & Jurkiewicz, 1999]. Particularly interesting is the rippled roof structure on the left, causing strong signal response. SAR simulation techniques are incorporated in the iterative building detection and reconstruction approach presented in the next chapter.

4. Approach for building detection and reconstruction from INSAR

4.1 Imagery and Ground Truth

A section of the captured test site (Karlsruhe, Germany) is shown in Fig. 7. During the SAR measurement an aerial image in oblique view was taken (Fig. 7a). The corresponding InSAR intensity and height are depicted in Fig. 7c,d. The range direction is bottom-up. The InSAR data is still in slant range geometry, with a better resolution in azimuth direction (horizontal coordinate). Fig. 7e shows the intensity image overlaid with the building footprints drawn by a human operator without any context information of the scene. This information shall be called “sensed truth”. The comparison with the LIDAR

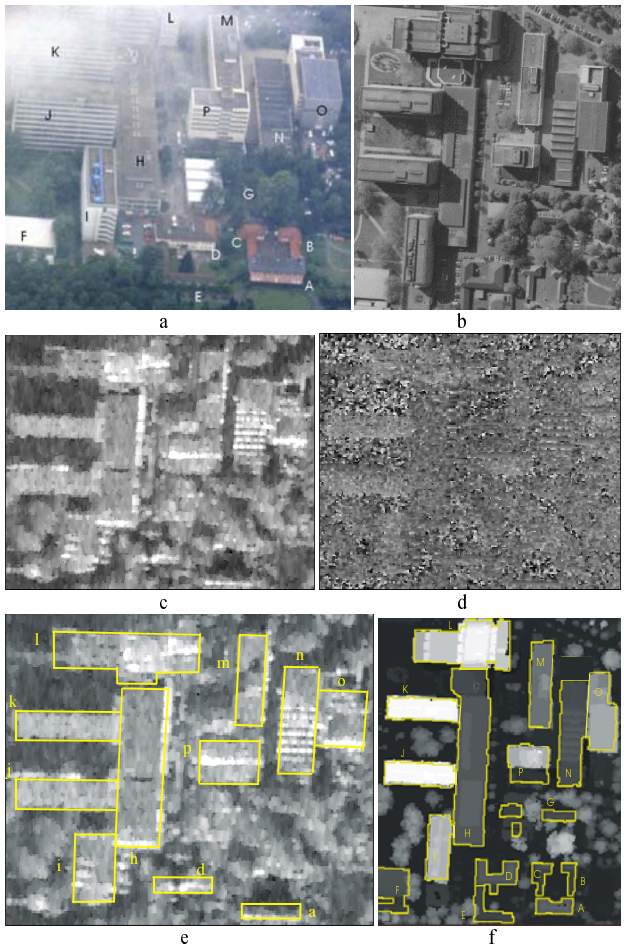

Figure 7. a) aerial image shot during InSAR measurement, b) aerial image in nadir view, c) InSAR intensity in slant range, d) InSAR height in slant range, e) “sensed truth”, f) LIDAR data and "ground truth”.

DEM (Fig. 7f) and the aerial image in nadir view (Fig. 7b) reveals that even a human operator cannot spot every building in the scene. Especially small buildings are hardly visible as are buildings which are covered by layover e.g. from high trees.

4.2 Algorithm overview

The building recognition is performed in an iterative manner. Detection and reconstruction of buildings is carried out in separated modules. The first step is the preprocessing of the InSAR data (e.g. smoothing and speckle reduction [Desnos & Matteini, 1993]). In the following segmentation step, primitive objects are extracted from the original slant range InSAR data. This is advantageous in order to avoid artifacts due to the geocoding, e.g. the distorted appearance of building edges in the ground range projection. From primitive objects, more complex objects (building hypotheses) are assembled in the detection step. After projection of coordinates of these building candidates from slant range into word coordinate system, a building recognition step follows. In this step model knowledge is exploited, e.g. rectangular shape of buildings or preferred parallel alignment of buildings along roads. Intermediate results are used for a simulation of layover, shadow and dihedral corner reflectors. The simulation results are re-projected to the SAR geometry and compared with the real data. Differences between the simulation and the real data steer the update of the process: new building hypotheses are generated and false ones eliminated. Hence, the resulting scene description is expected to converge to the real 3D objects in the scene with increasing number of steps.

4.3 Segmentation of primitive objects

Primitive objects are segmented in the intensity data and the height data.

Intensity Data: In the intensity data, edge and line structures are detected. There are three main types of structures of interest: (i) Salient bright lines caused from layover or double-bounce reflection. Those objects will be referred as objects STRONG_SCATTER_LINE. (ii) Edge structures at the border of a dark region which are potentially caused from building shadow. Two sets of objects are distinguished. The first set build those border edges of the dark region which face the sensor (object NEAR_SHADOW_EDGE). The other set consists of the edges at the far side of the dark region (object FAR_SHADOW_EDGE). (iii) The remaining edges build the set of other objects BUILDING_EDGE. Those may coincide with building edges orientated in range direction.

Height Data: In the height data, a segmentation of objects with significant elevation above ground is carried out. For this purpose a normalized DEM (NDEM) is derived from the InSAR height data, which represents the elevation of objects above ground. First a rank filtering of the height data is performed. The filter window size is chosen larger than the expected maximum building area. Height values coinciding with poor coherence or low intensity are not considered in this step in order to exclude blunders. This filtering results in a digital terrain model (DTM) representing the topography without elevated objects like trees or buildings. The NDEM is derived from the difference of the original InSAR height to the DTM. With an elevation threshold elevated objects are separated from the ground in the NDEM. Connected regions of elevated pixels build the set of objects ELEVATED_REGION.

4.4 Detection of Building Candidates in the Slant Range

From the line and edge structured primitive objects more complex objects QUADRANGLE are assembled by a production system: (i) At least one edge of the object QUADRANGLE facing the sensor must be derived from an object STRONG-SCATTER_LINE. (ii) Analogous, an object NEAR_SHADOW_EDGE is required at the far edges of the object quadrangle.
The objects QUADRANGLE from the test data are shown in Fig. 8. Only a subset of those coincide actually with buildings. A variety of different object configurations are source of false hints, e.g. fences or car rows etc.

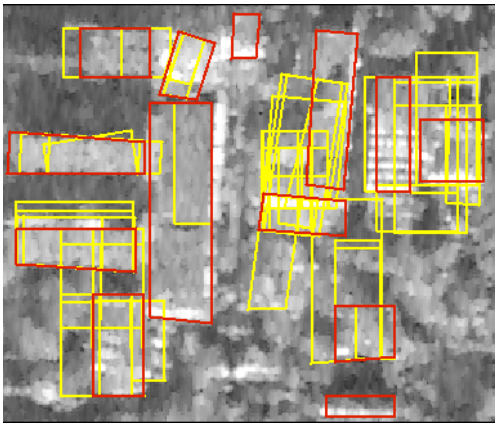

Figure 8. The set of all assembled objects quadrangle. The elevated and best assessed subset form the objects BUILDING_CANDIDATE (red)

For the discrimination of buildings from the rest, the objects ELEVATED_REGION are used. The intersection area of each object QUADRANGLE with all objects ELEVATED_REGION is determined. The ratio of the intersection area to the quadrangle area is used as object feature “elevated area ratio”. Only objects QUADRANGLE with an elevated area ratio larger than 0.7 are considered as objects BUILDING_CANDIDATE. The number of objects BUILDING_CANDIDATE is further reduced: from mutual intersecting candidates only the best assessed one is considered for the reconstruction step in this iteration. The assessment value depends on: (i) the overlap and the parallelism of the primitive objects and (ii) the

feature “elevated area ratio”. In Fig. 8 the remaining objects BUILDING_-CANDIDATE of the first iteration are drawn in red.

4.5 Building Reconstruction

The building reconstruction is based on the following scene model: (i) Footprints of buildings have rectangular or right-angled shape. (ii) Buildings are elevated objects with different roof structures. Three types of parametric building models are considered: flat roof buildings, gabled roof buildings and pent roof buildings. A common feature of the parametric building models is the rectangular footprint. (iii) A generic building model addresses complex buildings structures which consist of several parts like wings. These parts may have different height which is constant for each part. The footprint of a generic building is modeled as a right-angled polygon. The number of parts of a generic object is not a-priori determined. (iv) Neighboured buildings and the parts of complex buildings have often the same orientation, because they are aligned parallel to roads.

For the reconstruction step the coordinates of the objects BUILDING_-CANDIDATE are transformed from the SAR geometry into the world coordinate system. This step requires knowledge of the object height. A pixel by pixel transformation leads to distorted object edges, due to the noise sensitivity of the interferometric measurement. The noise impact is reduced by averaging the height values inside the borders of each object BUILDING_CANDIDATE. In case of a flat roofed building, the average value is the optimal estimate of the building height. In order to consider the different reliability of the height pixel values, the related coherence value is used as weight in the averaging procedure.

Because of tolerances in the building candidates assembly, the building footprint is usually not right-angled after geocoding. Therefore, the footprint is approximated by a rectangular or right-angled polygon. The roof structure is analysed with two different methods. The first method is restricted to the height data. After the re-projection of the right-angled building into the slant range, planes are fitted to the data. The second method analyzes the size and shape of the shadow areas (objects NEAR_SHADOW_EDGE and FAR_SHADOW_EDGE). Both results are combined to determine the roof shape and to improve the footprint location. The corrected footprint and roof structure are features of newly produced objects BUILDING.

4.6 Iterative improvement of the results

The first iteration is restricted to the reconstruction of objects BUILDING with rectangular footprints. In the following iterations the generic building model is considered as well. If several InSAR data sets are analyzed, the results are fused. In case of competing results, only the object BUILDING with the best assessment is accepted for the fused result. Occluded areas are filled and layover effects compensated. Due to parameter tolerances, the reconstructed orientations of neighbouring objects BUILDING might differ slightly. Hence, the orientations are corrected. The assessment of the objects buildings are used as weight for this adjustment step. Based on the intermediate results, simulations of layover, shadow and dihedral corner reflectors are carried out with respect of the parameters of the real data. Differences between the simulation and the real data are hints to inconsistencies. These govern the update of the process: new building hypotheses are generated and false ones eliminated. Then the reconstruction step is repeated.

5 Results

The result of the first iteration re-projected into the slant range after the reconstruction step is illustrated in Fig. 9a (red rectangles). The shadow analysis did not yield good results, due to the proximity of the buildings and many trees in the scene. Therefore, from the calculation of the building height based mainly on the InSAR height data, 13 buildings were detected. The result is assessed with respect to the two sets of ground truth data (Fig. 7e,f).

The comparison with the sensed truth (yellow in Fig. 9a) gives: 9 buildings are correct, one is missing (d) and one is over-segmented (l). The over-segmentation was caused from superstructures on the rooftop with significant different height. One false building is present (object 2) at the location of large trees. However, the major part of those buildings were detected which were labeled manually.

Fig. 9b illustrates the final result after five iterations. The grey level corresponds with the reconstructed building height. The real ground truth is superimposed in yellow. With respect to this ground truth, five additional buildings at the bottom of the scene are missing. The reason is, in most of the cases, occlusion or layover caused from high trees. Building G for example is not visible at all even in the aerial image shown in Fig. 3a. However, mainly small buildings were not detected. Especially, the height of tall buildings were underestimated. The buildings J and K on the left hand side are about 40 m high. But, their estimated height was 7 m smaller. A wrong height estimate leads to a erroneous position of the footprint after the forward transformation into the world coordinate system. The buildings appear shifted towards the sensor. The main parts of the two building complexes were detected. The recognition of the gabled roof of the small building A failed. It was reconstructed as flat roof building. This roof would not likely have been reconstructed correct from this InSAR data set even in the case that the building was detached. The reason is the orientation of the building in azimuth direction which is disadvantageous for the shadow analysis. For a illumination from the right, better results could be expected.

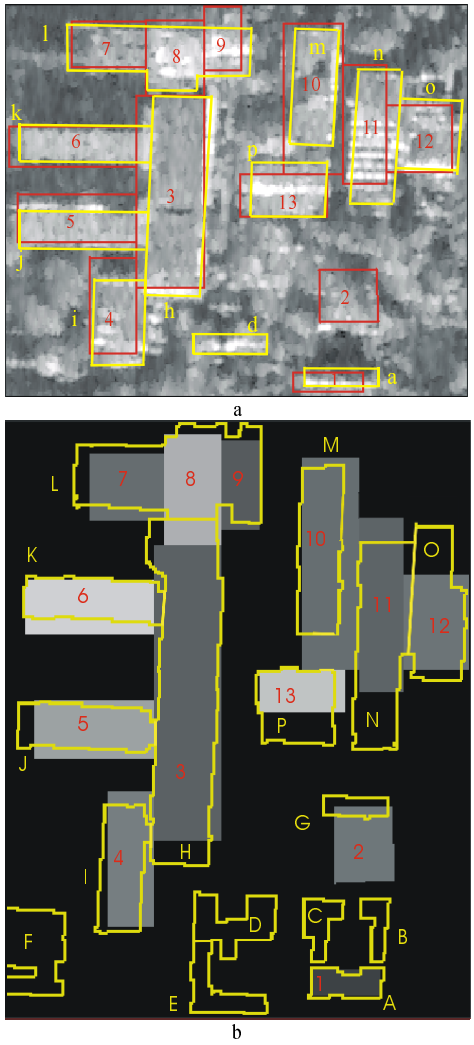

Figure 9. a) Result of first iteration re-projected into the slant range after the reconstruction step (red) and sensed truth, b) final result after 5 iterations (grey value coding of building height) superimposed with real ground truth.

6 Conclusion

The derived geometric relations show that some parts of the urban scene can not be sensed by a single SAR measurement. This behaviour is caused from the inherent side-looking illumination by SAR. The results of the approach confirm that especially tall buildings and trees may cause problem areas, due to occlusion or layover. However, the main buildings could be detected and reconstructed, even for the analysis of the given single InSAR data set. The accuracy of the results can not compete with 3D reconstructions derived from LIDAR data [Stilla & Jurkiewicz, 1999]. A potential for the improvement of results offers the fusion of several SAR and InSAR data [Bolter, 2001]. This has to be investigated with focus on dense urban areas. In case of a multi-aspect analysis an iterative approach is particularly suitable, because hints from one image may initiate a refined analysis at the related locations in the other images.

Acknowledgment

We want to thank Dr. Ender (FGAN-FHR Research Institute for High Frequency Physics and Radar Techniques) for providing the InSAR image data. The data were recorded by the AER II experimental system of FGAN.

References

Bolter R (2001) Buildings from SAR: Detection and reconstruction of buildings from multiple view high resolution interferometric SAR data, PhD. thesis, University Graz (Austria),

Desnos YL, Matteini V (1993) Review on structure detection and speckle filtering on ERS-1 images", EARSeL Advances in Remote Sensing, 2(2), 52-65.

Ender JHG (1998) Experimental results achieved with the airborne multi-channel SAR system AER-II. Proceedings of EUSAR'98, VDE, 315-318.

Gamba P, Houshmand B, Saccini M (2000) Detection and extraction of buildings from interferometric SAR data. IEEE Transactions on Geoscience and Remote Sensing, 38 (1): 611-618.

Meier E, Frei U, Nuesch D (1993) Precise terrain corrected geocoded images. In: Schreier G (ed) SAR geocoding: Data and systems. Karlsruhe: Wichmann, 173-185.

Schreier G (1993) Geometrical properties of SAR images. In: Schreier G (ed) SAR geocoding: Data and systems. Karlsruhe: Wichmann, 103-134.

Soergel U, Gross H, Thoennessen U, Stilla U (2000) Segmentation of interferometric SAR data for building detection. International Archives of Photogrammetry and Remote Sensing. Vol. 33, B1, 328-335

Soergel U, Schulz K, Thoennessen U, Stilla, U (2002) Utilization of 2D and 3D information for SAR image analysis in dense urban areas. Proc. EUSAR 2002, 429-434.

Stilla U, Jurkiewicz K (1999) Reconstruction of building models from maps and laser altimeter data. In: Agouris P, Stefanidis A (eds) Integrated spatial databases: Digital images and GIS. Berlin: Springer, 39-46.

Stilla U, Soergel U, Thoennessen U (2003) Potential and limits of InSAR data for building reconstruction in built-up areas. ISPRS Journal of Photogrammetry & Remote Sensing, 58 (2003) 113-123.